Antibiotic Optimization and Chemical Structure Stabilization of Thiomuracin A
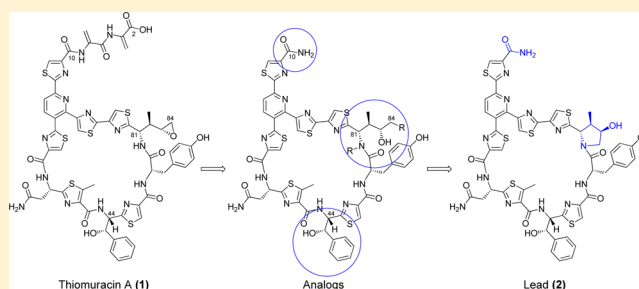
Matthew J. LaMarche,*,[†] Jennifer A. Leeds,[‡] Joanne Dzink-Fox,[‡] Eric Gangl,[†] Philipp Krastel,[⊥] Georg Neckermann,[‡] Deborah Palestrant,[§] Michael A. Patane,[†] Elin M. Rann,[†] Stacey Tiamfook,[‡] and Donghui Yu[‡]

[†]Global Discovery Chemistry, [‡]Infectious Disease Area, and [§]Protein Structure Unit, Novartis Institutes for Biomedical Research, Cambridge, Massachusetts 02139, United States
[⊥]Natural Products Unit, Novartis Institutes for Biomedical Research, Basel, Switzerland

Ⓢ *Supporting Information*

ABSTRACT: Synthetic studies of the antimicrobial secondary metabolite thiomuracin A (**1**) were initiated to improve chemical stability and physicochemical properties. Functional group modifications of **1** included removing the C2−C7 side chain, derivatizing the C84 epoxide region, and altering the C44 hydroxyphenylalanine motif. The resulting derivatives simplified and stabilized the chemical structure and were evaluated for antibacterial activity relative to **1**. The simplified structure and improved organic solubility of the derivatives facilitated isolation yields from fermentation broths and simplified the procedures involved for the process. These advancements increased material supply for continued medicinal chemistry optimization and culminated in the identification of **2**, a structurally simplified and chemically stable analogue of **1** which retained potent antibiotic activity.

■ INTRODUCTION

In 2009 we reported the fermentation, isolation, structural elucidation, antimicrobial activity, and biosynthetic gene cluster of a new class of thiazoyl actinomycetales metabolites, the thiomuracins (Figure 1).[1] These architecturally complex secondary metabolites, fermented from the rare soil actinomycetes species *Nonomurae*, are characterized by their highly modified, sulfur-containing macrocyclic peptide structures. The thiomuracins are structurally related to another class of actinomycetes metabolites, GE2270 A (**3**, Figure 1),[2] upon which we have based extensive drug discovery efforts.[3] Both the thiomuracins and **3** derive their antibiotic activity via binding to elongation factor Tu and disrupting prokaryotic protein synthesis. Currently, LFF571 (**4**), a derivative of **3**, is an investigational new drug in clinical trials for the treatment of *Clostridium difficile* infection.[4]

Clinical resistance to marketed drugs is becoming increasingly common.[5] Therefore, the discovery of antibiotics that act via novel mechanisms of action remains a high priority in infectious disease drug development. The thiomuracins possess potent antibiotic activity against methicillin-resistant staphylococci (MRSA), vancomycin-resistant enterococci (VRE), group A streptococci, and the anaerobic gut pathogen *Clostridium difficile*, with minimum inhibitory concentrations (MIC) < 1 μg/mL. This profile compared favorably to **3** and associated derivatives, specifically with respect to group A streptococci inhibition. Much like **3**, the poor physicochemical

properties of the thiomuracins (e.g., low solubility of the major fermentation metabolite, **1**) would require extensive optimization. The low solubility in organic solvents limited isolation yields from silica gel based chromatography. In addition, during fermentation and associated isolation processes, the C84 epoxide region was prone to undesired chemical transformations. Collectively, poor organic solubility and chemical decomposition complicated isolation and supply efforts.[1]

Due to our interest in the area of natural product based antimicrobial drug discovery[3] and the potent in vitro biological profile of the thiomuracins, we embarked on a medicinal chemistry optimization program. Our ability to build an antibiotic drug discovery program based on the thiomuracin scaffold would depend on two key factors: (1) stabilizing the C81−84 region of the structure to avoid undesired epoxide transformations and (2) increasing the organic solubility, which would facilitate purification, thereby increasing material supply for continued medicinal chemistry investigation. Herein, we describe the results of our effort directed toward improving these factors while retaining biological activity.

■ RESULTS

1 was available in high purity but in limited amounts (<100 mg) due to its limited chemical stability and challenges related
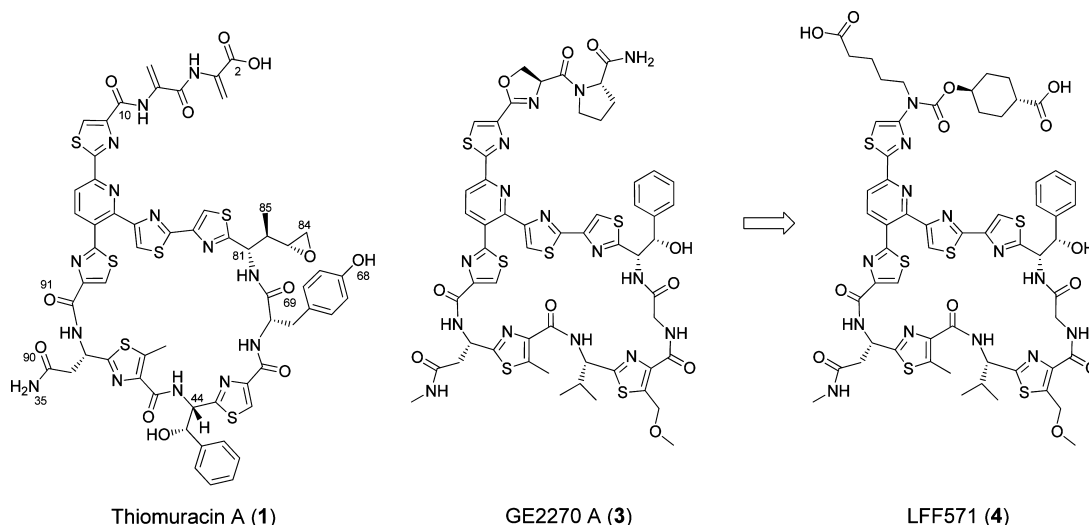
Figure 1. Structures of **1**, **3**, and **4**.

to purification.[1] However, the crude fermentation extract was available in multigram quantities and contained approximately 50% **1** by LCMS analysis. Initially, synthetic transformations designed to increase the organic solubility of **1** were conducted on the purified natural product. Ultimately, any prospective improvements would require demonstration on the crude extract itself. Simplifying the purification process and/or increasing the isolation yields of **1** (or an alternative, potent analogue) would constitute success.

Accordingly, the solubility of **1** was evaluated in a variety of solvents. DMSO and DMF emerged as the only solvents that would dissolve the material efficiently and reproducibly. The C2 carboxylic acid was selectively esterified under basic conditions (Scheme 1: Cs_2CO_3, MeI, DMF) in the presence of the two hydroxyls and the epoxide, which furnished **5**. Dissolution of methyl ester **5** easily proceeded in acetone, and the phenolic group was effectively alkylated (Cs_2CO_3, MeI, acetone), which afforded **6**. Thus, selective derivatization of the carboxylate and the phenol functionalities was achievable. Additionally, all hydroxyl groups in **5** were acetylated under standard conditions, which furnished analogue **7**. Unfortunately, when applying these protecting group protocols to the crude fermentation extract, the use of DMF as a solvent was ineffective, as product recoveries were low. We suspected that the low yields may be related to undesired side reactions of the C84 epoxide (vide infra). Additionally, troubleshooting reactions on the crude extract proved difficult because of the low purity of the starting material.

The sensitivity of **1** toward acid and base-mediated reactions was characterized as a means to understand possible decomposition pathways and overall chemical stability. Under acidic conditions (HCl, MeOH, H_2O) at room temperature, **1** proved quite stable (Scheme 2). When the temperature was elevated however (50 °C), the C2−C10 dehydroalanine-containing side chain was hydrolyzed and the epoxide ring was opened, affording the primary C10-thiazolyl amide chlorohydrin **6** in good yield. The chlorohydrin **6** was smoothly transformed into epoxide **7** under basic conditions (NaOH in MeOH/DCM, H_2O) and was further derivatized with base (NH_4OH) and under aqueous acidic conditions (TFA, H_2O) providing amine **8** and diol **9** analogues, respectively.

The chlorohydrin **8** and related derivatives were also treated with various organic bases (e.g., DBU, Scheme 3). These reactions cyclized N70 to C84 of the chlorohydrin to form a pyrrolidine. Protecting the alcohols first as acetates avoided competing epoxide formation and increased the yield of pyrrolidine cyclization. The acetates were then removed under standard conditions that afforded pyrrolidine **2**. Importantly, pyrrolidine **2** was chemically stable, soluble in mixtures of MeOH/DCM, and purified by flash chromatography with high recovery. Under forcing basic conditions (NH_4OH, 65 °C) however, the hydroxyl phenylalanine in the southern region was removed in a retroaldol-like fashion (inset) affording **12**, likely facilitated via thiazolyl stabilization at the pseudobenzylic C44 position. This undesired retroaldol reaction could be avoided by using mild temperatures. So a three-step synthetic protocol (acetylation, cyclization, and deprotection) could be efficiently executed on chlorohydrin **8** (itself resulting from crude extract acidic hydrolysis) as a one-pot procedure. Thus, the synthesis of a chemically stable, organic solvent soluble, and structurally simplified thiomuracin analogue **2** was accessible directly from the crude fermentation extract (ca. 50% **1**) in good overall yield (70%).

1 and novel analogues **2**, **5−12** were evaluated in MIC (minimum inhibitory concentration) assays for G+ bacteria growth inhibition. Five organisms comprised our antibacterial screen and included *Enterococcus faecalis*, *Enterococcus faecium*, *Staphylococcus aureus*, *Streptococcus pyogenes*, and the anaerobic intestinal pathogen, *Clostridium difficile*. *Streptococcus pneumonia* was also evaluated (not shown) but did not differ significantly from *S. pyogenes*. An in vitro transcription/translation cell extract assay was also employed to confirm that the analogues inhibited protein synthesis and to determine whether cellular penetration was affecting antibacterial activity.[6] **1** was potent in all five organisms tested with MICs ranging from 0.03 to 0.5 µg/mL. The protected analogues of **1** (i.e., **5**, **6**, and **7**) lost significant antibacterial activity (MICs: 1 to >32 µg/mL), which suggests that the carboxylic acid functionality and two hydroxyl groups located on the macrocycle may play important roles related to antibacterial activity. These analogues were inactive in the in vitro transcription/translation assay as well, which may be related to their low solubility (undeterminable). Surprisingly, the chlorohydrin and epoxy analogues with

**Scheme 1. Esterification and Hydroxyl Protection of 1**

Thiomuracin A (**1**)

Cs₂CO₃, MeI, DMF

DCM, DMAP, TEA

Cs₂CO₃, Acetone, H₂O, MeI

5

7

6
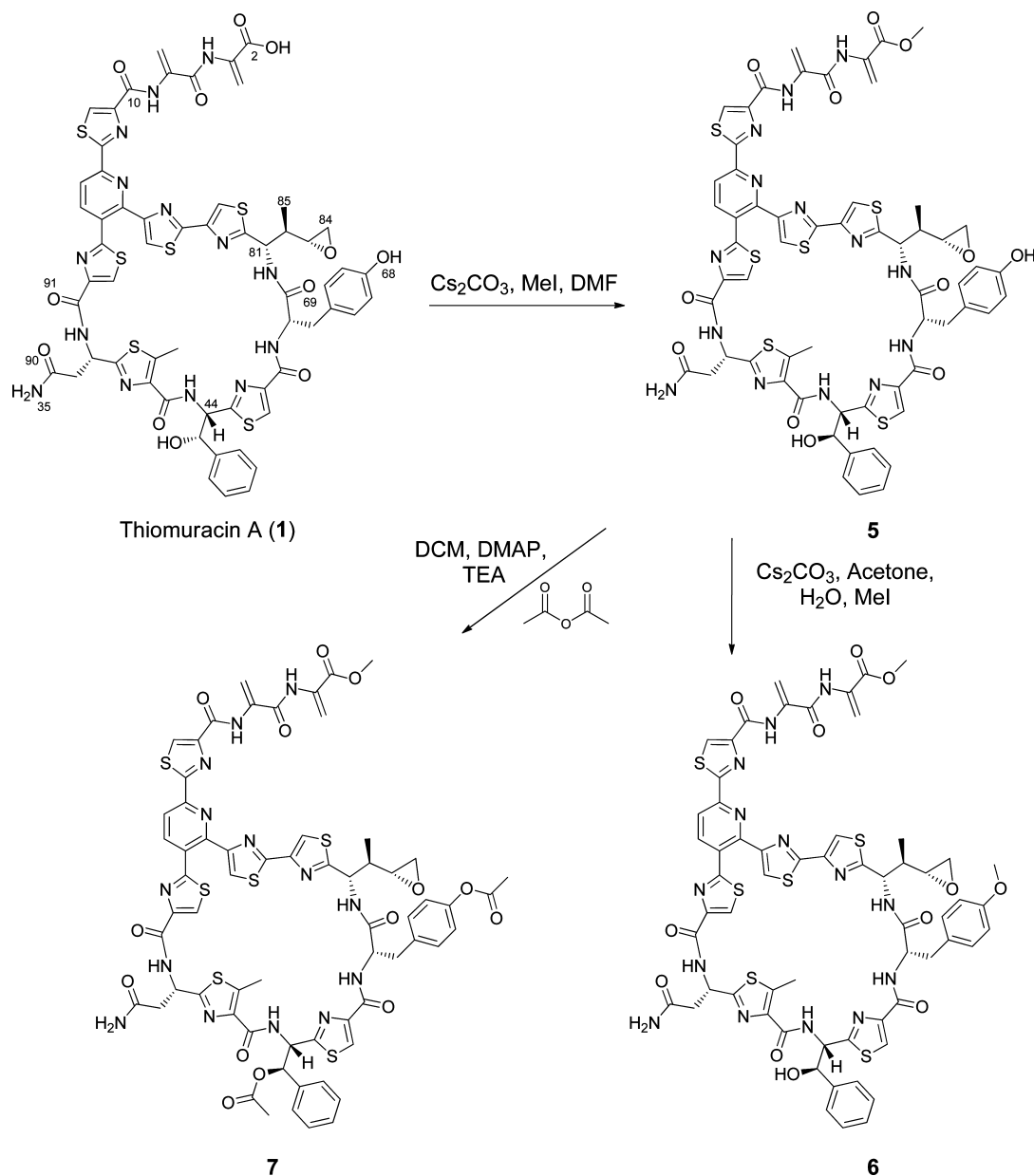
the C2−C10 side chain removed retained potent antibacterial activity in four out of five target organisms (i.e., **8**, **9**: MICs = 0.03−0.5 μg/mL). Group A streptococcus remained the least susceptible (**8**, **9**: MICs = 2 μg/mL). Furthermore, both amino and hydroxy derivatives of the epoxide (**10**, **11**, respectively) reduced the antibacterial activity as compared to the chlorohydrin **8**, while the retroaldol byproduct analogue **12** retained moderate activity in only three organisms (MIC = 2−4 μg/mL). The pyrrolidine **2** retained potent activity in all five target organisms with MICs ranging from <0.008 to 1 μg/mL. Importantly, analogues **8**−**12** and compound **2** retained activity in a transcription/translation assay measuring protein synthesis inhibition in cell extracts (50−75% inhibition @ 2uM). This data suggests that the observed SAR were likely due to differences in cellular penetration.

Thiomuracin derivative **2** was cocrystallized with *E. coli* EF-Tu at 2.3 Å (Figure 2, PDB code 4G5G). The homology between *E. coli* EF-Tu and *C. difficile* EF-Tu is high (86%

within 5 Å of the binding site). The macrocyclic conformation of **2** was quite similar as compared to **3** (PDB code 2C77), **4** (PDB code 3U2Q), and other derivatives of **3**, with intermolecular H-bond interactions noted between the primary amide (N35, thiomuracin numbering) and two residues (Asn273 and Phe296) and also the backbone nitrogen of Phe261 and O90 of thiomuracin. Further and unique interactions for **2** and the protein include intramolecular hydrogen bond stabilization between the tyrosine O68 and carbonyl O91 (3.1 Å) and also amide N35 and carbonyl O69 (3.0 Å). Phe218 also formed a T-stack interaction with the pyridine ring of **2**. In addition, the pyrrolidine methyl of **2** (C85) favorably fills the pocket formed by the side chain of Glu215. The pyrrolidine OH is also within reasonable hydrogen bonding distance (3.4 Å) with the Glu215 carboxylic acid. Interestingly, several functional groups appear to access solvent-exposed areas; these structural motifs may represent areas amenable to further derivatization for improved

**Scheme 2. Acid- and Base-Mediated Transformations of 1**
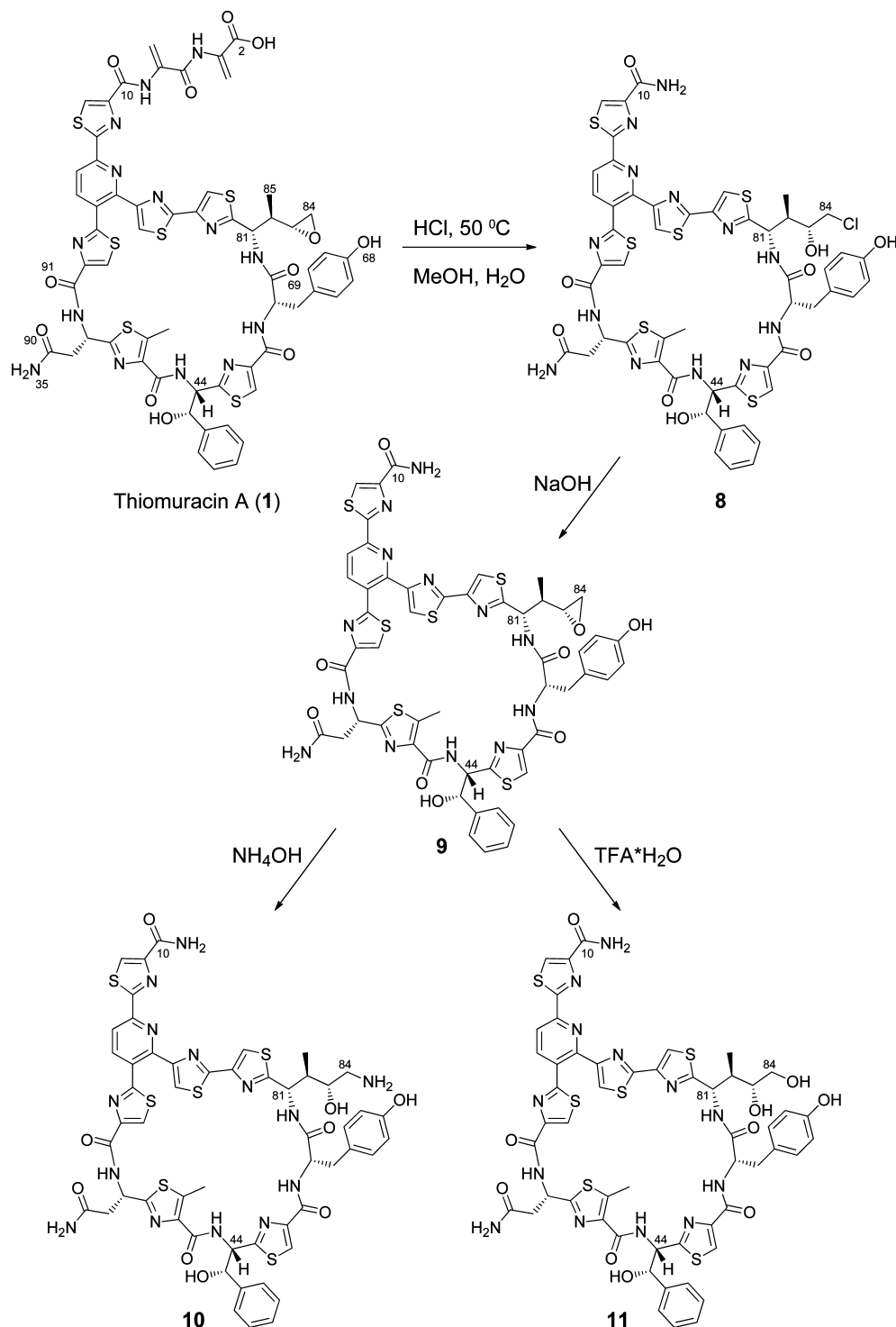
physicochemical properties. In particular, the hydroxyphenyla- lanine (O52), the pyrrolidine OH, and the amide (C10) all are oriented toward solvent.

Amide **2** was investigated in rat pharmacokinetic (Figure 3) and mouse efficacy experiments. Accordingly, **2** was dosed intravenously to male Sprague–Dawley rats (1 mg/kg).[7] Good systemic exposure (AUC = 1354 nM·h), low clearance (10.1 mL/min/kg), low volume of distribution (V_{ss} = 0.134 L/kg), and a moderate half-life ($T_{1/2}$ = 3.4 h) was observed. Furthermore, in a mouse systemic infection model,[8] amide **2**

displayed dose-dependent protection (via iv dosing) from lethal infection with ED_{50} values of 8.0 and 1.5 mg/kg against *S. aureus* and *E. faecalis*, respectively. Daptomycin was utilized as a positive control in these experiments; amide **2** proved to be less potent or commensurate depending on the organism (daptomycin: *S. aureus* ED_{50} = 0.3 mg/kg; *E. faecalis* ED_{50} = 3.3 mg/kg). Thus, amide **2** was more than 10-fold less active against *S. aureus* in the mouse systemic model as compared to daptomycin but 2-fold more potent against *E. faecalis*. These

Scheme 3. Pyrrolidine Cyclization
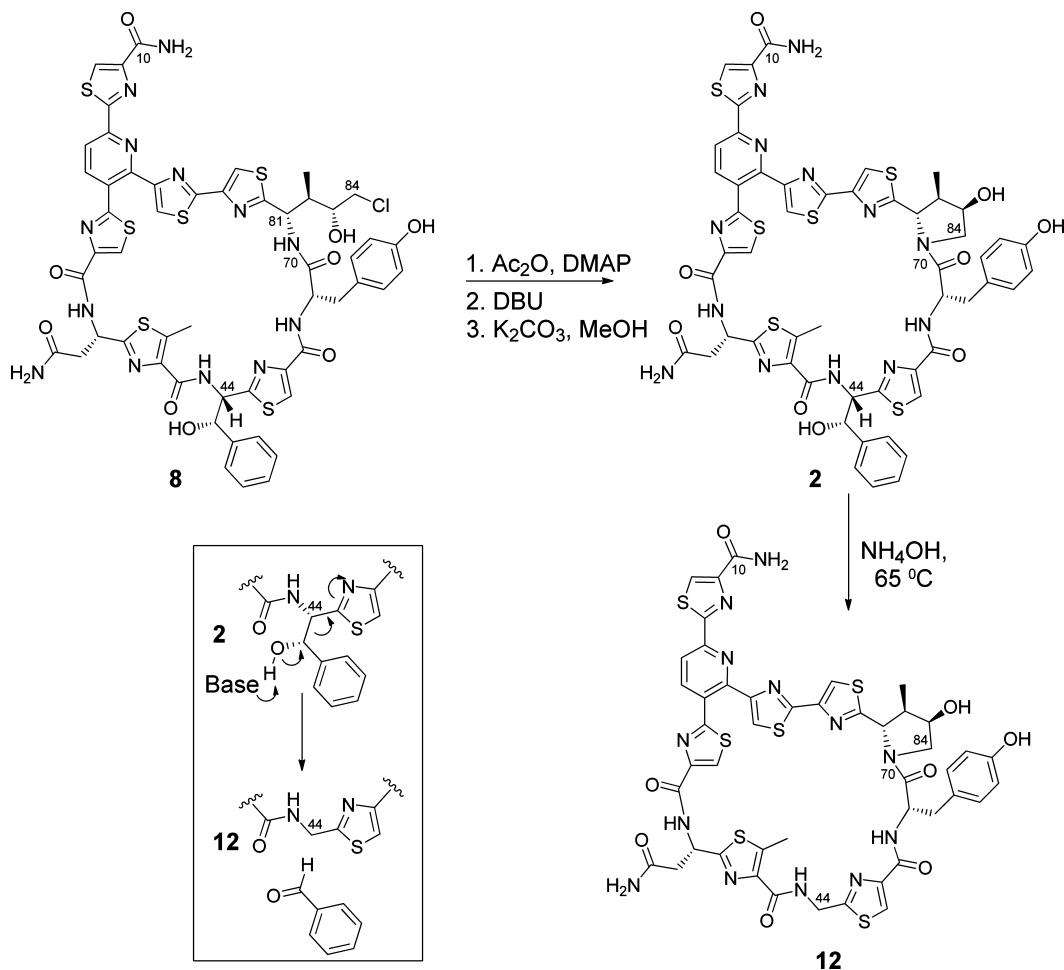
Table 1. Biological Activity of 1 and Analogues (MICs in μg/mL)

	1	2	5	6	7	8	9	10	11	12
E. faecalis	0.5	0.25	8	8	32	0.25	0.25	1	>32	4
E. faecium	0.5	0.5	8	8	32	0.5	0.125	1	>32	4
S. aureus	0.5	0.25	>32	>32	>32	0.5	0.5	2	>32	2
S. pyogenes	0.5	1	>32	>32	>32	2	2	>32	>32	>32
C. difficile	0.03	<0.008	1	1	>4	0.25	0.003	1	2	n/a

results also parallel results obtained with other derivatives of **3**.[3,4]

CONCLUSION

In summary, synthetic studies of the antimicrobial metabolite **1** were initiated to improve the chemical stability and physicochemical properties to facilitate isolation and material supply for further medicinal chemistry discovery. Novel semisynthetic analogues (**2**, **5−12**) of **1** included protecting group derivatives of hydroxyl and acid functionalities as well as derivatives stemming from acid- or base-mediated reactions. The latter resulted in the removal of the C2−C7 side chain, derivatization of the C84 epoxide region, and N70−C84 pyrrolidine cyclization. Most notably, removal of the C2−C10 side chain and cyclization of the C84 epoxide to a pyrrolidine (i.e., **2**) retained potent antibiotic activity in all five target Gram + organisms. The synthesis of pyrrolidine **2** was optimized (two pots, four steps) and demonstrated directly on the crude

fermentation extract, which facilitated overall material isolation and resupply. Amide **2** was also examined in pharmacokinetic studies and proved efficacious in the mouse systemic model of infection. Taken together, these studies culminated in the discovery of a structurally simplified, chemically stable analogue **2** of **1**, which retained antibacterial activity in vitro and in vivo, and allowed for continued medicinal chemistry exploration and optimization. The results of further SAR studies will be reported in due course.

EXPERIMENTAL SECTION

Compound Synthesis and Characterization. Synthetic procedures and compound characterization data are found in the Supporting Information. Compound purity was assessed by two distinct 20 min HPLC runs to confirm >95% purity.

MIC Assays. MIC assays were conducted according to broth microdilution methods described by the Clinical and Laboratory Standards Institute, Wayne, PA (CLSI M07-A8, 2009, Vol. 29, No. 2; CLSI M11-A7, Vol. 27). Bacterial strains included *E. faecalis* (ATCC
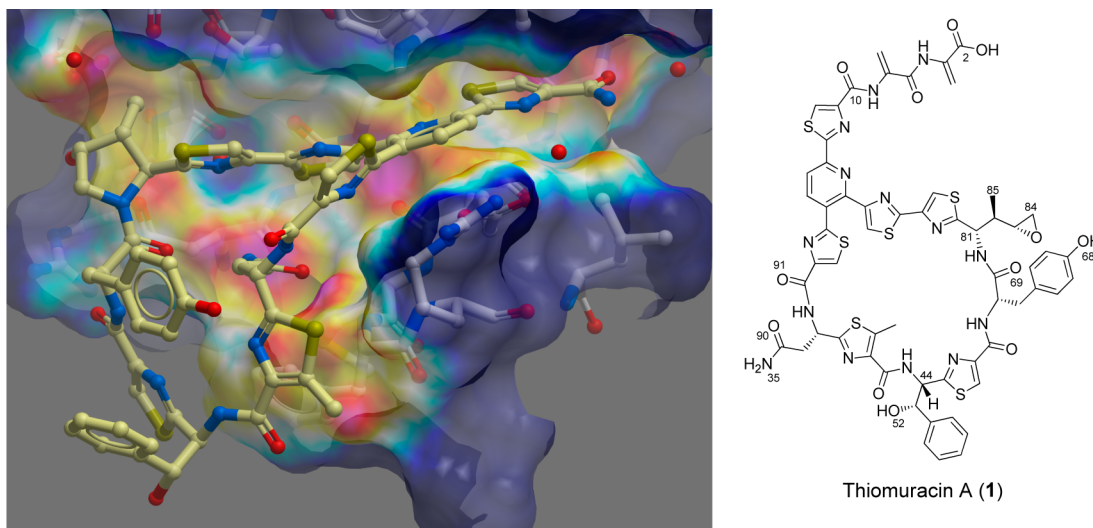
Figure 2. (a) Amide **2** cocrystyallized with *E. coli* EF-Tu at 2.3 Å. (b) Numbering of **1**.

	S. aureus	*E. faecalis*
2	8.0	1.5
Daptomycin	0.3	3.0

Figure 3. Efficacy profile of **2** in the mouse systemic infection model (EC_{50} in mg/kg).

29212), *E. faecium* (Prof. Chopra, Univ. Leeds UK, strain 7130724), *S. aureus* (MRSA from Prof. Willinger, isolated from a pharyngeal smear, AKH Vienna A4.018), *S. pyogenes* (ATCC BAA-595), and *C. difficile* (ATCC 43255).

In Vitro Transcription/Translation Assays. The *E. coli* S30 extract system for circular DNA (Promega cat. no. L1020) was used per recommendation of the manufacturer with slight modifications. Briefly, 3.5 μL of 286 ng/μL template DNA (pBESTluc) was mixed with 1.0 μL each of 1 mM "methionine minus" and "cysteine minus" amino acid mixes, 8 μL of S30 premix, 6 μL of S30 extract, and 0.5 μL of the test agents at 40× final concentration, in a total volume of 20 μL. The reaction mixtures were incubated for 2 h at 37 °C in 384-well flat bottom white plate (Corning, cat. no. 3704). The formation of luciferase was measured by adding an equal volume (20 μL) of Steady-Glo luciferase reagent (Promega cat. no. 27104), and emitted light was detected with a luminometer (Molecular Devices, LMaxll plate reader). Kirromycin and puromycin, which are known protein synthesis inhibitors, were used as positive controls. Ampicillin was used as a negative control. The Rabbit Reticulocyte TnT Quick Coupled Transcription/Translation system (Promega cat. no. L1170) was used as recommended by the manufacturer except that the assay volumes were scaled down from 50 to 20 μL. Briefly, the assay components consisted of 16 μL of TnT Quick master mix, 3 μL of (pT7luc) at 167 ng/μL, 0.5 μL of methionine, and 0.5 μL of the test compound at 40× final concentration in a final volume of 20 μL. The reaction mixtures were incubated at 37 °C for 75 min. Luminescence was detected as described above.

Rat Pharmacokinetic Studies. Intravenous PK studies ($N = 2$) were performed with male Sprague−Dawley rats, weighing 220−270 g and approximately 6−10 weeks old, which were obtained from Harlan Research Laboratories (South Easton, MA), each bearing dual implanted jugular vein cannula. The rats were fasted overnight before use and for 8 h after dosing. Blood samples were placed into K_2-EDTA-coated tubes and then centrifuged to yield plasma samples for analysis by LC-MSMS. Bioanalysis of rat plasma from in-life experiments were performed by LC-MSMS using a system with the following configuration: Agilent liquid chromatograph (Santa Clara, CA), LEAP Technologies CTC-PAL autosampler (Carrboro, NC), and Applied Biosystems API 4000 mass spectrometer (Framingham, MA). LC was performed in gradient mode with reversed phase C18

columns (2.1 mm × 30−50 mm × 3.5−5 μm particle size). The mobile phase A was 0.1% formic acid in water and mobile phase B was 0.1% formic acid in acetonitrile. Gradients were run from 5% B to 95% B in ~3.5 min. Plasma samples were protein-precipitated with acetonitrile containing glyburide as the internal standard (Sigma-Aldrich, St. Louis, MO).

Mouse Systemic Infection Model. The studies were approved by the Institutional Animal Care and Use Committee of the Novartis Institutes for BioMedical Research Inc., Cambridge MA. Animals were maintained under controlled conditions with free access to food and water. Female CD1 mice (21−25 g, Charles River Laboratories, Wilmington, MA) were used for infections with *S. aureus* (ATCC 49951) and *E. faecalis* (NB04025, a clinical isolate from the Novartis bacterial collection that is resistant to erythromycin, tetracycline, and gentamicin, courtesy of Dr. B. Willinger, Vienna General Hospital, Austria). MICs of amide **2** were 1 μg/mL and 0.125 μg/mL for animal strains *S. aureus* (ATCC 49951) and *E. faecalis* (NB04025), respectively. Lethal infections were induced by intraperitoneal injection of a freshly prepared bacterial suspension of 1×10^8 CFU/mouse in either 50% sterile rat fecal extract (*E. faecalis*) or 0.9% NaCl (*S. aureus*). The injected bacterial dose corresponded to 10−100 times the minimal lethal dose as determined from previous lethal dose titration studies. Against *E. faecalis* infections the mice were treated once immediately following the bacterial inoculation, while against *S. aureus* infections mice were treated 1 and 5 h after inoculation. Compound **2** was formulated in 5% DMA, 30% PEG400, 10% cremophor EL, 5% 0.1 N NaOH, 50% pH 7.4 buffer. Daptomycin was formulated in saline. Compounds were administered iv via tail vein bolus injection at several dose levels to groups of six mice each. Following bacterial inoculation, the mice were observed for 5 days. In addition, body temperature was monitored by electronic micro-transponders (Bio Medic Data Systems, Inc., Seaford, DE) that were implanted in mice subcutaneously prior to infection. Mice that became moribund as indicated by a combined score based on clinical observations and drop in body temperature were preemptively euthanized. The 50% effective dose (ED_{50}), the dose providing protection to 50% of mice, and the 95% confidence limits (95% CI) were calculated from the survival data at day 5 by probit analysis using the program Systat (SPSS Inc.). All animals in the vehicle-treated control groups developed lethal infections.

Crystallization and X-ray of Compound 2·EF-Tu Complex. To form the EF-Tu·NVP-compound **2** complex, 10 mg/mL (227 μM) *E. coli* EF-Tu protein in a buffer containing 50 mM Tris pH 8 and 50 mM NaCl was incubated with 1 mM compound **2** for 1 h at 4 °C. The sample was centrifuged at 20 000g to remove any resulting precipitate. Crystallization was carried out using 300 nL of the protein sample plus 300 nL of crystallization solution containing 0.1 mM Tris pH 8.23,

24% PEG3350, 0.2 M MgSO$_4$, using a sitting drop format and equilibrated against a reservoir of the crystallization solution. The crystal was flash frozen with liquid nitrogen after being stabilized in a cryobuffer containing 0.1 mM Tris pH 8.23, 24% PEG3350, 0.2 M MgSO$_4$, 20% ethylene glycol.

X-ray Data Collection. Initial data from a single crystal of the EF-Tu·compound **2** complex were collected on a ADSC Quantum 210 CCD detector using synchrotron radiation (λ = 1 Å) at the IMCA-CAT beamline 17-ID of the Argonne Photon Source. Data were collected using φ rotations of 0.5° and 180° of total data collected.

X-ray Data Processing, Structure Determination, and Refinement. Data from the EF-Tu·compound **2** complex were processed using the HKL2000 Suite, version 0.95.[9] Data processing statistics are shown in Table 2. Crystals were diffracted to 2.3 Å

Table 2

	compound **2**
data collection parameters (highest resolution shell)	
resolution range (Å)	50−2.3 (2.38−2.3)
total observations	148 584
unique reflections	21 195
completeness (%)	99.7 (100)
I/σ	44.8 (8.0)
R_{sym}	0.073
refinement parameters	
R_{work}/R_{free}	0.212/0.258
protein atoms	3047
heterogen atoms (Mg/GDP/compd)	87
solvent atoms	117
average B-factor (Å^2)	43.6
rms Deviations from ideal value	
bond lengths (Å)	0.009
bond angles (deg)	1.6

resolution in the space group $P2(1)2(1)2$ with a unit cell of a = 80.305 Å, b = 123.577 Å, c = 45.092 Å, $\alpha = \beta = \gamma = 90°$. Data collection statistics are shown in Table 2. The structure of the EF-Tu·GDP·compound **2** complex was determined by the molecular replacement as implemented in PHASER,[10] using *E. coli* EF-Tu protein as a search model (1D8T). The resulting molecular replacement solution contained one EF-Tu·GDP·compound **2** protein complex in the asymmetric unit. Refinement was carried out with CNX[11] using a single round of rigid-body refinement, following several cycles of simulated annealing refinement, B-factor refinement, and model building with the COOT software package.[12] Water molecules, GDP, and the Mg^{2+} ion were added prior to addition of the ligand **2**. Refinement produced a final model with excellent geometry (rmsd bond lengths 0.009 Å, rmsd bond angles 1.6°) and R-factors of R_{work} and R_{free} of 21% and 26%, respectively.

■ ASSOCIATED CONTENT

Ⓢ Supporting Information

Detailed synthetic procedures and compound characterization data. This material is available free of charge via the Internet at http://pubs.acs.org.

■ AUTHOR INFORMATION

Corresponding Author

*Tel: (617) 871-7729. Fax: 617-871-4081. E-mail: matthew.lamarche@novartis.com.

Notes

The authors declare no competing financial interest.

■ ABBREVIATIONS USED

MIC, minimum inhibitory concentration; EC$_{50}$, 50% effective dose; G+, Gram positive; MRSA, methicillin-resistant *Staphylococcus aureus*; VRE, vancomycin-resistant enterococci; *S. aureus*, *Staphylococcus aureus*; *E. faecalis*, *Enterococcus faecalis*; *E. faecium*, *Enterococcus faecium*; *S. pyogenes*, *Streptococcus pyogenes*; EF-Tu, elongation factor-Tu

■ REFERENCES

(1) Morris, R. P.; Leeds, J. A.; Naegeli, H. U.; Oberer, L.; Memmert, K.; Weber, E.; LaMarche, M. J.; Parker, C. N.; Burrer, N.; Esterow, S.; Hein, A. E.; Schmitt, E. K.; Krastel, P. *J. Am. Chem. Soc.* **2009**, *131*, 5946−5955.

(2) Selva, E.; Beretta, G.; Montanini, N.; Saddler, G. S.; Gastaldo, L.; Ferrari, P.; Lorenzetti, R.; Landini, P.; Ripamonti, F.; Goldstein, B. P.; Berti, M.; Montanaro, I.; Denaro, M. *J. Antibiot.* **1991**, *44* (7), 693−701. The structure was later corrected and verified: Tavecchia, P.; Gentili, P.; Kurz, M.; Sottani, C.; Bonfichi, R.; Selva, E.; Lociuro, S.; Restelli, E.; Ciabatti, R. *Tetrahedron* **1995**, *51* (16), 4867−4890 . For acidic decomposition, see above.

(3) (a) LaMarche, M. J.; Leeds, J. A.; Dzink-Fox, J.; Gunderson, K.; Krastel, P.; Memmert, K.; Patane, M. A.; Rann, E. M.; Schmitt, E.; Tiamfook, S.; Wang, B. 4-Aminothiazolyl Analogues of GE2270 A: Antibacterial Lead Finding. *J. Med. Chem.* **2011**, *54*, 2517−2521. (b) LaMarche, M. J.; Leeds, J. A.; Dzink-Fox, J.; Mullin, S.; Patane, M. A.; Rann, E. M.; Tiamfook, S. 4-Aminothiazolyl Analogues of GE2270 A: Design, Synthesis, and Evaluation of Imidazole Analogs. *Bioorg. Med. Chem. Lett.* **2011**, *21* (2011), 3210−3215. (c) LaMarche, M. J.; Leeds, J. A.; Brewer, J. T.; Bushell, S. M.; Dewhurst, J. M.; Dzink-Fox, J.; Gangl, E.; Jain, A.; Mullin, S.; Neckermann, G.; Osborn, C.; Palestrant, D.; Patane, M. A.; Rann, E. M.; Sachdeva, M.; Shao, J.; Tiamfook, S.; Whitehead, L.; Yu, D. Antibacterial Optimization of 4-Aminothiazolyl Analogues of GE2270 A: Identification of the Cycloalkylcarboxylic Acids. *J. Med. Chem.* **2011**, *54*, 8099−8109.

(4) LaMarche, J. M.; Leeds, J. A.; Amaral, A.; Brewer, J. T.; Bushell, S. M.; Deng, G.; Dewhurst, J. M. ; Ding, J.; Dzink-Fox, J.; Gamber, G.; Jain, A.; Lee, K.; Lee, L.; Lister, T.; McKenney, D.; Mullin, S.; Osborne, C.; Palestrant, D.; Patane, M. A.; Rann, E. M. ; Sachdeva, M.; Shao, J.; Tiamfook, S.; Trzasko, A.; Whitehead, L.; Yifru, A.; Yu, D.; Yan, W.; Zhu, Q. Discovery of LFF571: An Investigational Agent for *Clostridium difficile* Infection. *J. Med. Chem.* **2012**, *55*, 2376−2387.

(5) Poulakou, G.; Giamarellou, H. *Expert Opin. Investig. Drugs* **2007**, *16* (2), 137−155.

(6) (a) Zubay, G. In *Vitro Synthesis of Protein in Microbial Systems*. *Annu. Rev. Genet.* **1973**, *7*, 267−287. (b) Zubay, G. Isolation and Properties of CAP, the Catabolite Gene Activator. *Methods Enzymol.* **1980**, *65*, 856−877.

(7) Because of the lack of aqueous solubility, organic excipients were necessary to enable formulation of **2** (5% DMA, 30% PEG400, 10% cremophor EL, 5% 0.1 N NaOH, 50% pH 7.4 buffer).

(8) Frimodt-Moller, N.; Knudesen, J. D.; Espersen, F. *Handbook of animal models of infection*; Zak, O.; Sand, M. A., Eds.; Academic Press: San Diego, 1999; pp 127−136. O'Reilly, T.; Cleeland, R.; Squires, E. L. *Antibiotics in laboratory medicine*, 4th ed.;Lorian, V., Ed.; Williams & Wilkins: Baltimore, 1996; pp 604−765.

(9) Otwinowski, Z.; Minor, W. Processing of X-ray Diffraction Data Collected in Oscillation Mode. In *Methods in Enzymology*; Carter, C. W., Jr.; Sweet, R. M., Eds.; Academic Press: New York, 1997; Vol. 276: Macromolecular Crystallography, part A, pp 307−326.

(10) McCoy, A. J.; Grosse-Kunstleve, R. W.; Adams, P. D.; Winn, M. D.; Storoni, L. C.; Read, R. J. Phaser crystallographic software. *J. Appl. Crystallogr.* **2007**, *40*, 658−674.

(11) Brünger, A. T.; Adams, P. D.; Clore, G. M.; DeLano, W. L.; Gros, P.; Grosse-Kunstleve, R. W.; Jiang, J. S.; Kuszewski, J.; Nilges, M.; Pannu, N. S.; Read, R. J.; Rice, L. M.; Simonson, T.; Warren, G. L. Crystallography & NMR system: A new software suite for macromolecular structure determination. *Acta Crystallogr., Sect. D: Biol. Crystallogr.* **1998**, *54* (Pt 5), 905−921.

(12) Emsley, P.; Cowtan, K. Coot: model-building tools for molecular graphics. *Acta Crystallogr., Sect. D: Biol. Crystallogr.* **2004**, *60*, 2126−2132.